

Coherent manipulation of a single magnetic atom using polarized single electron transport in a double quantum dot

Wenxi Lai and Wen Yang

Beijing Computational Science Research Center, Beijing 100094, China

(Received 24 February 2015; revised manuscript received 11 September 2015; published 27 October 2015)

We consider theoretically a magnetic impurity spin driven by polarized electrons tunneling through a double-quantum-dot system. The spin-blockade effect and spin conservation in the system make the magnetic impurity sufficiently interact with each transferring electron. As a result, a single collected electron carries information about spin change of the magnetic impurity. The scheme may develop all-electrical manipulation of magnetic atoms by means of single electrons, which is significant for the implementation of scalable logical gates in information processing systems.

DOI: [10.1103/PhysRevB.92.155433](https://doi.org/10.1103/PhysRevB.92.155433)

PACS number(s): 76.30.Da, 42.50.Dv, 72.25.Pn, 73.23.Hk

I. INTRODUCTION

Magnetic atoms are critical spin systems which have potential applications in data storage and quantum information processing [1–3]. In particular, using electrons to manipulate magnetic atoms is a natural step towards the implementation of scalable memory units for future integrated circuits. In dilute II–VI semiconductor quantum dots (QD), interaction between a manganese atom and a carrier can be effectively described with the *sp-d* exchange interaction [4–6]. Based on the impurity-carrier coupling, electrical control of the single magnetic atom is feasible by injecting different charges in the magnetic atom-doped QD [6].

As shown both in experiment [2] and theory [7], electrons can directly tunnel through a Mn atom by taking its spin states. The ground state and excited states of the Mn atom can be identified with the current since they support different conductances. However, in the tunneling from a scanning tunneling microscope tip to Cu₂N surface through an individual Mn atom, the Mn spin spontaneous relaxation is more frequent than excitation by tunneling electrons [2]. Compared with the case in high-dimensional bulk material, the lifetime of the Mn spin is much longer in a QD [8]. Therefore, coherent electrical manipulation of the Mn spin is possible in a low-dimensional nanostructure. In a QD doped with a single Mn atom, charge and conductance of the single electron tunneling can be related to the spin state of the Mn atom [9]. However, it is hard to exactly connect a quantum state of the magnetic atom to a single electron in the above QD system, which is a problem that should be solved for future quantum information processing.

In this paper, we propose a scheme for all-electrical manipulation of the magnetic impurity spin, scaling the number of driving electrons down to one. To this end, we consider two intercoupled semiconductor QDs, in which one QD contains a single magnetic impurity and couples to a spin-polarized electron source. The other QD is localized in a homogeneous magnetic field and connected to a normal conductance, playing the role of a spin filter. In previous studies [2,6,7,9], electrons were transported through the magnetic atom without any qualification to their spins; as a result, interaction between the magnetic atom and electrons was very weak. In contrast, the QD spin filter induces spin-dependent tunneling, which makes sure each electron would be completely flipped by the magnetic atom before it passes through the filter. Therefore,

each collected electron can be correlated with the change of spin state in the magnetic atom. There are several facts that are very beneficial for the realization of our scheme. First, two coupled QDs can be fabricated, with doping of a single magnetic ion in one of them [10]. Second, spin lifetime of an electron in II–VI semiconductor quantum dots can be long enough. Electron relaxation time in a similar system was reported to be 50 ns in a previous work [11]. In a QD embedded in a magnetic atom, a longer lifetime of around 1 μ s was predicted [12]. Third, a magnetic atom such as Mn impurity with a relaxation time from 1 μ s to 0.4 ms was observed in experiment [10,13]. The time is longer than the driving time of the magnetic atom, which will be shown later. Fourth, the technique for real-time detection of single electron tunneling has been well developed recently [14–17]. Fifth, polarized electron current is available from several sources, for instance, a QD spin splitter under the premise of local magnetic field [18,19], ferromagnetic leads [20,21], and graphene or carbon atom wires [22,23]. Recently, nuclear spins of donor atoms such as phosphorus and ²⁹Si have been coherently controlled and read using bounded electrons in these donors and the spin-to-charge conversion. Electromagnetic field was applied to initialize these nuclear spins [24–26]. In comparison with these early works, the main advance in our present protocol is that the magnetic atom will be manipulated all electrically. In other words, a magnetic atom can be controlled using only a single electron transistor without the application of any electromagnetic field. Even the initialization of the impurity spin can be progressed using the single electron tunneling in principle.

II. MODEL AND THEORY

Our model is illustrated in Fig. 1. The two QDs are denoted by dot 1 and dot 2 with ground orbital levels ε_1 and ε_2 , respectively. Both electron polarization in the left lead and the external magnetic field \vec{B} applied on dot 2 are assumed to be parallel to the QD growth direction z . Electrons injected from the left lead into dot 1 are coupled to the magnetic atom by the ferromagnetic Heisenberg-type spin-exchange interaction. We describe the spin of the magnetic atom with the mean value of the spin along the z direction $\langle \hat{M}_z \rangle$, where \hat{M} is the magnetic atom spin operator and the brackets indicate the

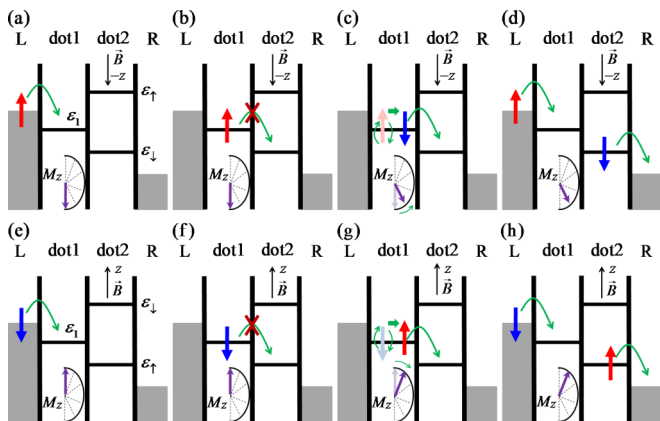


FIG. 1. (Color online) Schematic illustration of the principle in our model. In (a)–(d) the applied magnetic field is in the down direction and up polarized electrons are injected into the double QD. In (e)–(h), the external magnetic field is changed to be the up direction, and down polarized electrons are injected.

average over quantum states of the system. Bias voltage and the magnetic field is tuned so that just the lowest levels of the two QDs fall within the bias window $\mu_L > \varepsilon_1, \varepsilon_\downarrow$ (or ε_\uparrow) $> \mu_R$, where the indexes \downarrow, \uparrow indicate electron states with spin up and down, respectively. In addition, the intradot Coulomb blockade energies U_1, U_2 corresponding to dots 1 and 2 are assumed to be much larger than other energy scales, which indicates that only single electron occupation is involved in either of the QDs. It remarkably simplifies our model and calculation.

In Figs. 1(a)–1(d), the magnetic field in this configuration is applied along the $-z$ direction with value $\vec{B} = (0, 0, -B)$. It means, in dot 2, the ground-state level is $\varepsilon_\downarrow = \varepsilon_2 - g^* \mu_B B/2$ and the first excited level is $\varepsilon_\uparrow = \varepsilon_2 + g^* \mu_B B/2$, where g^* is the Landé g factor of the electron in the QD and μ_B is the Bohr magneton. The system requires spin-up electrons that are injected from the left lead into dot 1. We take energy levels that satisfy $\varepsilon_\uparrow > \mu_L$ and $\varepsilon_\uparrow - \varepsilon_1 \gg \hbar\Omega$, where $\hbar\Omega$ is the interdot coupling strength. This energy structure forms a spin-conditioned repulsive potential which ensures that the spin-up electron is forbidden to enter dot 2 until its spin is flipped to be upside down due to its coupling to the magnetic atom. As soon as the electron spin would change to down, it would be allowed to pass through dot 2 and collected in the right lead. At the same time, the spin of the magnetic atom would change from $\langle \hat{M}_z \rangle$ to $\langle \hat{M}_z \rangle + \hbar$. If a spin-down electron is injected from the left lead, it directly moves through the double dots without any change in the spin of the magnetic atom. However, if the left lead is a fully up polarized electron source, each passed electron would be connected to the spin change of the magnetic atom. In this case, due to spin conservation, if the spin of the magnetic atom is changed from $\langle \hat{M}_z \rangle$ to $\langle \hat{M}_z \rangle + n_\downarrow \hbar$, then the number of electrons detected in the right lead should equal n_\downarrow , and their spins are down polarized.

The magnetic atom can also be driven in the reverse, which is presented in Figs. 1(e)–1(h). Since the magnetic field is turned to be in the z direction here, the spin filter allows only spin-up electrons to tunnel through dot 2. The input electrons are required to be in the spin-down state, and output electrons

are expected to be in the spin-up state. Each transported electron contributes to the spin of the magnetic atom with the value $-\hbar$. It yields the reverse impurity magnetization orientation, which means the spin of the magnetic atom would be changed from $\langle \hat{M}_z \rangle$ to $\langle \hat{M}_z \rangle - n_\uparrow \hbar$ with the collection of n_\uparrow spin-up electrons.

To give a quantitative description of the model, we use the following Hamiltonian [5,27]:

$$\hat{H} = \hat{H}_{d1} + \hat{H}_{d2} + \hat{H}_{d12} + \hat{H}_{\text{lead}} + \hat{H}_{\text{tun}}, \quad (1)$$

where the Hamiltonian for dot 1 is

$$\hat{H}_{d1} = \varepsilon_1 \hat{n}_1 + U_1 \hat{n}_{1\uparrow} \hat{n}_{1\downarrow} - j_e \vec{M} \cdot \vec{S}_1 \quad (2)$$

and the Hamiltonian for dot 2 is

$$\hat{H}_{d2} = \varepsilon_2 \hat{n}_2 + U_2 \hat{n}_{2\uparrow} \hat{n}_{2\downarrow} + g^* \mu_B \vec{B} \cdot \vec{S}_2. \quad (3)$$

The interdot tunneling Hamiltonian reads

$$\hat{H}_{d12} = \hbar\Omega(\hat{n}_{12} + \hat{n}_{12}^\dagger) + U \hat{n}_1 \hat{n}_2. \quad (4)$$

Here, $\hat{n}_i = \hat{n}_{i\uparrow} + \hat{n}_{i\downarrow}$, $\hat{n}_{i\uparrow} = \hat{c}_{i\uparrow}^\dagger \hat{c}_{i\uparrow}$, $\hat{n}_{i\downarrow} = \hat{c}_{i\downarrow}^\dagger \hat{c}_{i\downarrow}$, $\hat{n}_{12} = \hat{n}_{12\uparrow} + \hat{n}_{12\downarrow}$, $\hat{n}_{12\uparrow} = \hat{c}_{1\uparrow}^\dagger \hat{c}_{2\uparrow}$, $\hat{n}_{12\downarrow} = \hat{c}_{1\downarrow}^\dagger \hat{c}_{2\downarrow}$. $\hat{c}_{i\uparrow}$ ($\hat{c}_{i\downarrow}$) is the annihilation operator of a spin-up (spin-down) electron in dot i ($i = 1, 2$). S_1 and S_2 represent electron spin in dots 1 and 2, respectively. U is the interdot Coulomb potential. The exchange coupling strength between the electron in dot 1 and the magnetic atom is given by $j_e = J |\psi_0(r_M)|^2$ with exchange integral J and the electron ground-state wave function ψ_0 at the magnetic impurity position r_M .

The left and right electronic leads are described by the free-electron baths with the Hamiltonian

$$\hat{H}_{\text{lead}} = \sum_{k,\sigma;\alpha=L,R} \varepsilon_{\alpha k} \hat{c}_{\alpha k\sigma}^\dagger \hat{c}_{\alpha k\sigma}. \quad (5)$$

Dot 1 is coupled to the left leads, and dot 2 is coupled to the right lead by

$$\hat{H}_{\text{tun}} = \sum_{k,\sigma} V_L \hat{c}_{Lk\sigma}^\dagger \hat{c}_{1\sigma} + \sum_{k,\sigma} V_R \hat{c}_{Rk\sigma}^\dagger \hat{c}_{2\sigma} + \text{H.c.}, \quad (6)$$

with the left and right tunneling amplitudes V_L and V_R , respectively.

Time evolution of electron transport through the double QD system is described by a quantum master equation which is derived based on the Hamiltonian (1) and the Liouville–von Neumann equation in the Born-Markov approximation. Since the transport in our system is a process of single electron sequential tunneling through QDs and works in the weak-tunneling regime, the master equation is an effective approach to describe our model [28–30]. The equation of motion is given in terms of the reduced density matrix $\hat{\rho}$ of the system,

$$\frac{\partial}{\partial t} \hat{\rho} = \frac{1}{i\hbar} [\hat{H}_{d1} + \hat{H}_{d2} + \hat{H}_{d12}, \hat{\rho}] + \hat{\mathcal{L}}_L \hat{\rho} + \hat{\mathcal{L}}_R \hat{\rho}. \quad (7)$$

The Liouville superoperators, $\hat{\mathcal{L}}_L$ and $\hat{\mathcal{L}}_R$, acting on the density matrix $\hat{\rho}$ describe tunneling on the left and right sides of the double dots, respectively. They are written as

$$\begin{aligned} \hat{\mathcal{L}}_L \hat{\rho} = & \frac{1}{2} \sum_{\sigma} \Gamma_L^{\sigma} [f_{L,\sigma} (\hat{c}_{1\sigma}^\dagger \hat{\rho} \hat{c}_{1\sigma} - \hat{c}_{1\sigma} \hat{c}_{1\sigma}^\dagger \hat{\rho}) \\ & + (1 - f_{L,\sigma}) (\hat{c}_{1\sigma} \hat{\rho} \hat{c}_{1\sigma}^\dagger - \hat{c}_{1\sigma}^\dagger \hat{c}_{1\sigma} \hat{\rho}) + \text{H.c.}] \quad (8) \end{aligned}$$

and

$$\hat{\mathcal{L}}_R \hat{\rho} = \frac{1}{2} \sum_{\sigma} \Gamma_{R,\sigma}^{\sigma} \hat{f}_{R,\sigma} (\hat{c}_{2\sigma}^{\dagger} \hat{\rho} \hat{c}_{2\sigma} - \hat{c}_{2\sigma} \hat{c}_{2\sigma}^{\dagger} \hat{\rho}) + (1 - \hat{f}_{R,\sigma}) (\hat{c}_{2\sigma} \hat{\rho} \hat{c}_{2\sigma}^{\dagger} - \hat{c}_{2\sigma}^{\dagger} \hat{c}_{2\sigma} \hat{\rho}) + \text{H.c.}, \quad (9)$$

where the Fermi distribution function in the left lead is $\hat{f}_{L,\sigma} = \{\exp[(\varepsilon_1 + U_1 \hat{n}_{1\bar{\sigma}} - \mu_L)/k_B T] + 1\}^{-1}$ and that in the right lead is $\hat{f}_{R,\sigma} = \{\exp[(\varepsilon_{\sigma} + U_2 \hat{n}_{2\bar{\sigma}} - \mu_R)/k_B T] + 1\}^{-1}$, depending on the charging energy U_i conditioned by the occupation, $n_{i\bar{\sigma}} = c_{i\bar{\sigma}}^{\dagger} c_{i\bar{\sigma}}$, of an electron with spin $\bar{\sigma}$. Here, the spin index $\bar{\sigma}$ is defined so that if $\sigma = \uparrow(\downarrow)$, then $\bar{\sigma} = \downarrow(\uparrow)$. The tunneling rates are spin dependent and are given by $\Gamma_{\alpha}^{\uparrow} = \Gamma_{\alpha}(1 + P_{\alpha})/2$ and $\Gamma_{\alpha}^{\downarrow} = \Gamma_{\alpha}(1 - P_{\alpha})/2$, with the current polarization $P_{\alpha} = (I_{\alpha}^{\uparrow} - I_{\alpha}^{\downarrow})/(I_{\alpha}^{\uparrow} + I_{\alpha}^{\downarrow})$. Here, I_{α}^{σ} is a current with pure spin σ on the side of α ($\alpha = L, R$). The bare tunneling rates can be expressed as $\Gamma_{\alpha} = 2\pi \hbar |t_{\alpha}|^2 N_{\alpha}(\varepsilon)$ with the density of states $N_{\alpha}(\varepsilon)$ of electrons at energy ε .

III. MANIPULATION OF A MAGNETIC ATOM WITH SPIN $M = 5/2$

The Hilbert space of the double QD system is generated by the basic vectors $|i\rangle_1 |m\rangle_1 |j\rangle_2$, where $|i\rangle_1$ and $|j\rangle_2$ represent electronic states in dot 1 and dot 2, respectively. Here, $i, j = 0$ denote the empty state, $i, j = \downarrow, \uparrow$ indicate occupation states of a single electron with spin down and spin up, respectively. $|m\rangle_1$ is the eigenstate of the impurity spin operator \hat{M}_z with eigenvalues $m = -M, -M + 1, \dots, M$.

First, we consider a typical single magnetic atom which displays a spin of $M = 5/2$ in the QD, such as Fe or Mn. These magnetic atoms have six quantized spin states $|m\rangle$, with corresponding eigenvalues $m = -5/2, -3/2, -1/2, 1/2, 3/2, 5/2$ [4]. In Fig. 2(a), the initial state $|\psi_M(0)\rangle$ of the magnetic atom is set to be any of the six quantized states. In all cases the magnetic atom is driven to the final state $|5/2\rangle$. On average, the value of the Mn spin $\langle M_z \rangle = \text{Tr}[\hat{M}_z \hat{\rho}]$ trace is taken over

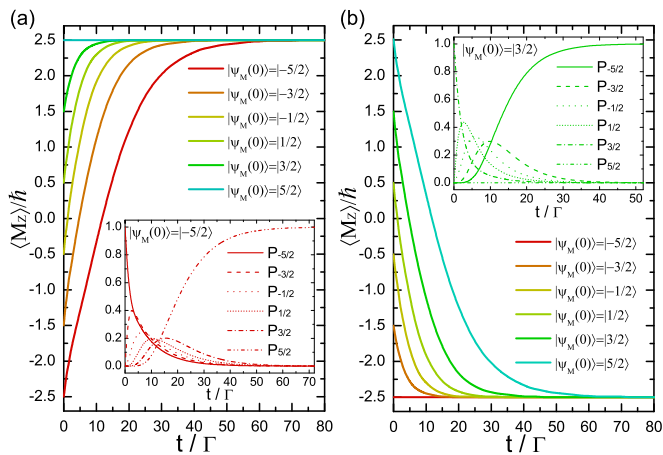


FIG. 2. (Color online) Time evolution of the single impurity magnetization as a function of time. (a) The applied external magnetic field is $\vec{B} = (0, 0, -B)$. (b) The applied external field is $\vec{B} = (0, 0, B)$. The Parameters are $\mu_L = 75\Gamma$, $\mu_R = -75\Gamma$, $\varepsilon_1 = 0$, $\varepsilon_2 = 62.5\Gamma$, $g^* \mu_B B = 135\Gamma$, $j_e = 3\Gamma$, $k_B T = 12.5\Gamma$, $\Gamma_L = \Gamma_R = \Gamma$, $P_R = 0$, $\hbar\Omega = 5\Gamma$, $U = 10\Gamma$.

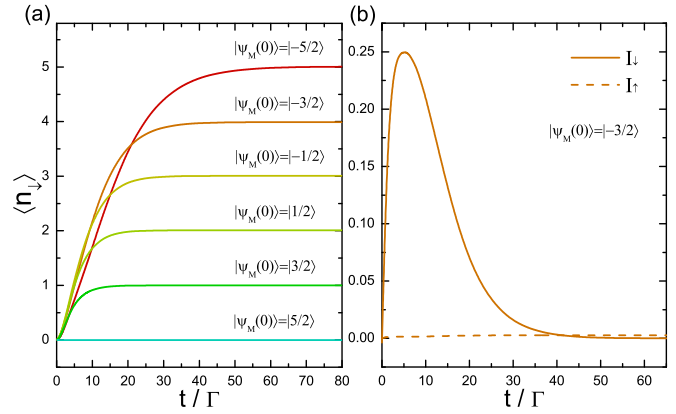


FIG. 3. (Color online) (a) The number of spin-down electrons collected in the right side of the system. (b) Current for spin-up and spin-down electrons as a function of time. The parameters are the same as those in Fig. 2.

the basic vectors $|i\rangle_1 |m\rangle_1 |j\rangle_2$. When the impurity spin changes to $|5/2\rangle$, it becomes parallel to the injected electron spin, and there will be no spin flip in the later time. Then the electron tunneling should be switched off, and the spin-down polarized current decreases to zero, as plotted in Fig. 3(b). The figures also show that orientation time of the Mn spin is a few tens of nanoseconds when one takes a tunneling characteristic time of $\Gamma^{-1} \sim 1$ ns. It is comparable to the time scale of a previously reported optical control [13]. Since each electron contributes to the spin change of the magnetic atom with momentum \hbar , the magnetic atom initialized in states $|\psi_M(0)\rangle = |-5/2\rangle, |-3/2\rangle, |-1/2\rangle, |1/2\rangle, |3/2\rangle, |5/2\rangle$ leads to finite electrons collected in the right lead with definite numbers $\langle n_{\downarrow} \rangle = 5, 4, 3, 2, 1, 0$, respectively. The number of electrons collected in the right lead can be seen in Fig. 3(a) for corresponding initial spin states. The collected electron number is calculated using the formula

$$\langle n_{\sigma} \rangle = \frac{1}{e} \int_0^{\infty} I_{\sigma}(t) dt, \quad (10)$$

where $I_{\sigma}(t)$ is the current on the right side of dot 2. The current is derived from the charge fluctuating in the two dots, $d(\langle n_1 \rangle + \langle n_2 \rangle)/dt = \sum_{\sigma=\uparrow, \downarrow} (I_L^{\sigma} - I_R^{\sigma})/e$ with the replacement $I_{\sigma}(t) = I_R^{\sigma}$. The reversal time evolution of the magnetization is shown in Fig. 2(b).

IV. MANIPULATION OF A MAGNETIC ATOM WITH SPIN $M = 1/2$

Now, we consider a magnetic ion with spin $M = 1/2$, such as Cu^{2+} . This kind of impurity has the particular meaning that its maximum magnetization difference is \hbar , from $-\hbar/2$ to $\hbar/2$ or vice versa. In this case, only a single electron is involved in the tunneling. As shown in Fig. 4(a), when we set the initial state of the magnetic atom to be $|1/2\rangle$, it is transformed into $|1/2\rangle$. At the same time, the up polarized current is changed to a down polarized current after interacting with the magnetic atom. The down polarized current is expected to be collected on the right side, which is characterized by a single electron with spin down, as shown in Fig. 4(b). To show the collected charge is really limited, the average current as a function of time is

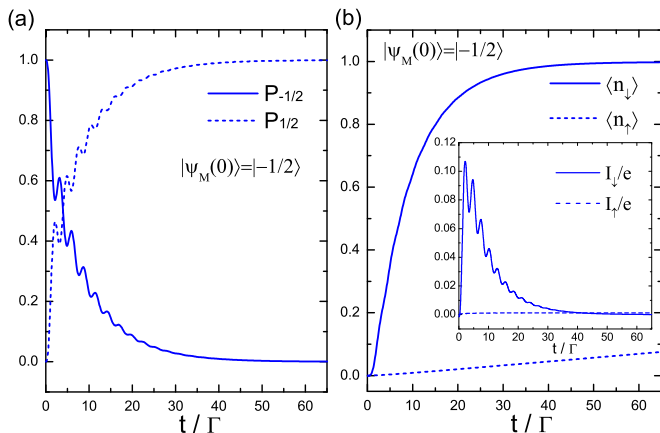


FIG. 4. (Color online) (a) Probabilities of the magnetic atom in its spin states $| -1/2 \rangle$ and $| 1/2 \rangle$. The magnetic atom is initially in the state $| -1/2 \rangle$. (b) The number of collected electrons with spin up and spin down corresponding to the case in (a). The parameters are $\mu_L = 70\Gamma$, $\mu_R = -70\Gamma$, $\varepsilon_1 = 0$, $\varepsilon_2 = 57.5\Gamma$, $g^* \mu_B B = 125\Gamma$, $j_e = 2\Gamma$, $k_B T = 10\Gamma$, $\Gamma_L = \Gamma_R = \Gamma$, $P_L = 1$, $P_R = 0$, $\hbar\Omega = 3\Gamma$, $U = 10\Gamma$.

plotted in the inset of Fig. 4(b). The down polarized current sharply increases and then disappears slowly with a small fluctuation. The up polarized current is negligibly weak. From the point of application, the double-QD system embedded a magnetic atom with spin $M = 1/2$ is a very good system for data storage, where only a single electron of current and the two states of the magnetic atom are correlated.

The small fluctuation in the current occurred due to the back-action from the system. Since charge transfer through the double dots requires electron spin flip, the amplitude of the current is proportional to the rate of electron spin change. The rate of spin change is determined by the strength of spin coupling between the magnetic atom and electrons. Therefore, we can deduce that the oscillations observed in Fig. 4 are caused by the coherent coupling between the magnetic atom and an individual electron. Indeed, the character of the small oscillation can be tuned by changing the spin coupling strength j_e . Actually, the back-action effect can also be seen in the former situation for $M = 5/2$. However, considering six spin states of the magnetic atom are involved in the exchange interaction and the larger couplings j_e and Ω are taken, the small oscillation during the evolution of the spin states and current is too smooth to be observed.

The above results are described in a relatively ideal situation. Now, let's talk about some more practical cases. Figure 5(a) reveals that an increase in the interdot tunneling strength excites a spin-up electron from dot 1 into the excited level ε_\uparrow of dot 2, which leads to the unexpected spin-up electron leakage from the double dot system into the right lead. To restrain the electron leakage through the excited level ε_\uparrow , we suggest that one can take a relatively small interdot coupling $\hbar\Omega$, which is required to be much smaller than the decoupling $\varepsilon_\uparrow - \varepsilon_1$.

The system is also sensitive to polarization of the right lead. Figure 5(b) shows that when the polarization is not pure, the number of electrons collected in the right lead is larger than

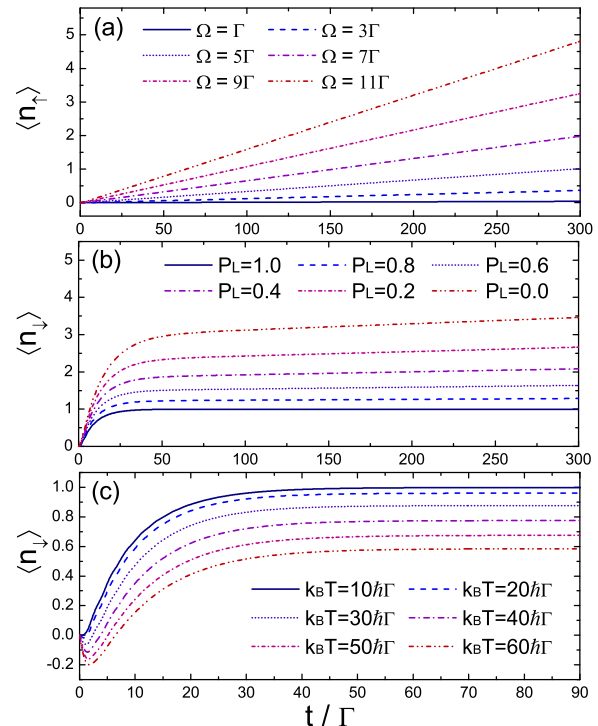


FIG. 5. (Color online) (a) Number of spin-up electrons collected in the right side of the double QD with different interdot coupling strengths, $k_B T = 10\Gamma$, $P_L = 1$. (b) Number of spin-down electrons for different spin polarizations in the left lead, $k_B T = 10\Gamma$, $\hbar\Omega = 3\Gamma$. (c) Number of collected spin-down electrons at different temperatures, $\hbar\Omega = 3\Gamma$, $P_L = 1$. The rest of the parameters are the same as those in Fig. 4.

the expected value. Since nonpurely polarized current contains electrons with different spin orientations, some electrons could not be blocked by dot 2.

The negative number of electrons in Fig. 5(c) implies that electrons in the right lead have a certain probability to flow into the QDs at the beginning of tunneling due to the thermal excitation since the QDs are empty initially. After the system reaches steady state, the higher the temperature is, the larger the electron distribution is in the QDs. The electrons staying in the QDs come from the leads. Therefore, the net number of electrons collected in the right lead decreases when temperature increases.

V. DISCUSSION

In experiment, realizing electron transport through a magnetic atom-doped II–VI semiconductor QD is still a challenge. There are some well-developed experimental backgrounds, for instance, spin-dependent electron transport through a quantum well containing dilute magnetic material [31] and resonant tunneling through a CdSe self-assembled QD with Mn ions [32]. In addition, an attempt to orient a Mn spin using the charge transported from a neighboring QD has been successfully realized [10].

Creating a local magnetic field is a key technical problem for the experimental implementation of our proposal. The left lead is a polarized electron source, so an external magnetic

field may be required on it. In addition, the right QD needs a magnetic field to create a Zeeman splitting for an electron. At the same time, these magnetic fields must have a negligible effect in the left QD and the right lead. Therefore, some local magnetic fields are necessary in the nanostructure. To this end, a proper quantity of external magnetic field can be exerted on the left lead for the generation of a spin-polarized electron source. As the QD is a zero-dimensional nanoscale system, our suggestion is to use a magnetic grain, such as Co grain [33,34], to create magnetic field on the right QD. To explore its effectiveness we estimate the field strength of a typical Co grain, which consists of hundreds of atoms. We assume the Co grain is a uniformly magnetized sphere. Then, the field of the grain can be obtained from the formula $B = \frac{2}{3}\mu_0\mathbb{M}$, where μ_0 is permeability of free space and \mathbb{M} is magnetization of the grain [35]. We assume that average magnetic moment per Co atom is $1.5\mu_B$. In real materials the local magnetic moment is always larger than this value [33]. We assume the diameter of a Co atom is about 0.15 nm. Then, the magnetic field of the Co grain is estimated to be not less than $B = 6.6T$. By increasing size of the Co grain, a stronger field can be obtained. In a CdTe semiconductor QD, the corresponding Zeeman splitting of an electron reaches $|g^*\mu_B B| = 0.64$ meV, where the g factor is given by $g^* = -1.67$ in this material [36]. To guarantee the left QD and the right lead are not significantly influenced by the surrounding magnetic field, magnetic shielding may be applied here to protect the spreading field. One kind of magnetic shielding material is a superconducting chip which expels magnetic field via the Meissner effect. Another kind of shielding material is a certain high-permeability metal alloy which, in contrast to the superconductor, draws the field into itself. Using an example with the high-permeability shielding with permeability μ , the field in the shielded volume is $\frac{9b^3\mu_0}{2(b^3-a^3)\mu}$ times smaller than the outside field [37]. For the convenience of quantitative estimation, the shielding material here is assumed to be a spherical shell with inner radius a and outer radius b . When the permeability μ is large enough, adequate shielding of the field in the shielded area can be achieved. In practice, as the QD couples to an electronic reservoir and another dot, the shielding material may not be absolutely closed with a lower efficiency.

In the Hamiltonian in our model, spin-exchange interaction between the two QDs is not considered. In fact, when each quantum dot contains one electron, the exchange interaction does not play an important role in the whole system. The reason is that the electron in dot 2 has a definite spin direction. It has to gain a large amount of energy to change spin. However, it is hard for the electron in dot 1 to provide a large amount of energy. In addition, the system is robust against the double occupancy in dot 1. Since current injected from the left lead is assumed to be purely spin polarized, two electrons with different spin states in dot 1 do not break the spin conservation

as soon as dot 2 is set to output electrons with pure spin, whereas double occupancy in dot 2 induces spin leakage and, as a result, the correlation between electrons and the magnetic atom becomes weak. However, considering the high Coulomb blockade effect in either of the QDs, double occupancy in any dot is negligibly small in our model.

The characteristic times of an information processing system are very significant. There are two kinds of critical times; one of them is manipulation time τ_s of the system, and the other is lowest lifetime bound τ_i of these information carriers, such as the magnetic atom and electrons. The manipulation time of the system indicates a time range during which an electron is emitted from the left lead and then collected in the right lead; at the same time control of the magnetic atom is accomplished. It is clear that spin lifetimes of the information carriers are required to be at least longer than the manipulation time of the system, i.e., $\tau_i > \tau_s$. As mentioned in the Introduction, a single Mn spin relaxation time from 1 μ s to 0.4 ms in a CdTe QD [10,13] and an electron lifetime from 50 ns to 1 μ s in II–VI semiconductor systems are reported. Even in a QD including certain charges, the Mn atom relaxes on a time scale of about 100 ns [38]. As shown in Secs. III and IV, the manipulation time of the system is about 50 ns for a characteristic time of the electron tunneling, $\Gamma^{-1} \sim 1$ ns. Furthermore, there is still space for reducing the manipulation time of the system. Actually, properly increasing the dot-reservoir coupling (electron tunneling rate) or interdot coupling would improve the rate of the control process. In this case, a lower bound of the spin lifetime is allowed.

VI. CONCLUSIONS

In the system, change of the magnetic impurity spin is correlated with the spin state and the number of single electrons that tunnel through the two QDs. Based on this principle, we give the following conclusions: (i) Our model works as an electron source in which the number of emitted electrons can be determined beforehand by setting an initial state of the magnetic atom or using a magnetic atom with certain spin M . In particular, a single electron emitter is available using a magnetic atom with spin 1/2. (ii) The number of polarized transferring electrons can be recorded in the spin state of the magnetic atoms. (iii) The change in the spin state of the magnetic atom should be detected by counting the number of electrons emitted from the double QDs. (iv) The spin state of the magnetic impurity can be controlled, in principle, by injecting a suitable number of spin-polarized electrons, and this control is reversible.

ACKNOWLEDGMENT

We appreciate the valuable discussion with S. Zhang about the numerical calculation.

-
- [1] L. Thomas, F. Lioni, R. Ballou, D. Gatteschi, R. Sessoli, and B. Barbara, *Nature (London)* **383**, 145 (1996).
 [2] S. Loth, K. von Bergmann, M. Ternes, A. F. Otte, C. P. Lutz, and A. J. Heinrich, *Nat. Phys.* **6**, 340 (2010).

- [3] R. Hanson and D. D. Awschalom, *Nature (London)* **453**, 1043 (2008).
 [4] L. Besombes, Y. Léger, L. Maingault, D. Ferrand, H. Mariette, and J. Cibert, *Phys. Rev. Lett.* **93**, 207403 (2004).

- [5] D. E. Reiter, T. Kuhn, and V. M. Axt, *Phys. Rev. B* **85**, 045308 (2012).
- [6] Y. Léger, L. Besombes, J. Fernández-Rossier, L. Maingault, and H. Mariette, *Phys. Rev. Lett.* **97**, 107401 (2006).
- [7] F. Delgado, J. J. Palacios, and J. Fernández-Rossier, *Phys. Rev. Lett.* **104**, 026601 (2010).
- [8] M. Scheibner, T. A. Kennedy, L. Worschech, A. Forchel, G. Bacher, T. Slobodskyy, G. Schmidt, and L. W. Molenkamp, *Phys. Rev. B* **73**, 081308 (2006).
- [9] J. Fernández-Rossier and R. Aguado, *Phys. Rev. Lett.* **98**, 106805 (2007).
- [10] M. Goryca, T. Kazimierzczuk, M. Nawrocki, A. Golnik, J. A. Gaj, P. Kossacki, P. Wojnar, and G. Karczewski, *Phys. Rev. Lett.* **103**, 087401 (2009).
- [11] D. H. Feng, I. A. Akimov, and F. Henneberger, *Phys. Rev. Lett.* **99**, 036604 (2007).
- [12] M. D. Petrović and N. Vukmirović, *Phys. Rev. B* **85**, 195311 (2012).
- [13] C. Le Gall, L. Besombes, H. Boukari, R. Kolodka, J. Cibert, and H. Mariette, *Phys. Rev. Lett.* **102**, 127402 (2009).
- [14] J. Bylander, T. Duty, and P. Delsing, *Nature (London)* **434**, 361 (2005).
- [15] W. Lu, Z. Ji, L. Pfeiffer, K. W. West, and A. J. Rimberg, *Nature (London)* **423**, 422 (2003).
- [16] S. Gustavsson, R. Leturcq, M. Studer, I. Shorubalko, T. Ihn, K. Ensslin, D. C. Driscoll, and A. C. Gossard, *Surf. Sci. Rep.* **64**, 191 (2009).
- [17] J. P. Pekola, O.-P. Saira, V. F. Maisi, A. Kemppinen, M. Möttönen, Y. A. Pashkin, and D. V. Averin, *Rev. Mod. Phys.* **85**, 1421 (2013).
- [18] P. Recher, E. V. Sukhorukov, and D. Loss, *Phys. Rev. Lett.* **85**, 1962 (2000).
- [19] R. Hanson, L. M. K. Vandersypen, L. H. W. van Beveren, J. M. Elzerman, I. T. Vink, and L. P. Kouwenhoven, *Phys. Rev. B* **70**, 241304(R) (2004).
- [20] P. Hyde, L. Bai, D. M. J. Kumar, B. W. Southern, C.-M. Hu, S. Y. Huang, B. F. Miao, and C. L. Chien, *Phys. Rev. B* **89**, 180404 (2014).
- [21] A. Dirnacher, M. Grifoni, A. Prüfling, D. Steininger, A. K. Hüttel, and C. Strunk, *Phys. Rev. B* **91**, 195402 (2015).
- [22] Z. Y. Li, W. Sheng, Z. Y. Ning, Z. H. Zhang, Z. Q. Yang, and H. Guo, *Phys. Rev. B* **80**, 115429 (2009).
- [23] V. M. Karpan, G. Giovannetti, P. A. Khomyakov, M. Talanana, A. A. Starikov, M. Zwierzycki, J. van den Brink, G. Brocks, and P. J. Kelly, *Phys. Rev. Lett.* **99**, 176602 (2007).
- [24] J. J. Pla, K. Y. Tan, J. P. Dehollain, W. H. Lim, J. J. L. Morton, D. N. Jamieson, A. S. Dzurak, and A. Morello, *Nature (London)* **489**, 541 (2012).
- [25] J. J. Pla, K. Y. Tan, J. P. Dehollain, W. H. Lim, J. J. L. Morton, F. A. Zwanenburg, D. N. Jamieson, A. S. Dzurak, and A. Morello, *Nature (London)* **496**, 334 (2013).
- [26] J. J. Pla, F. A. Mohiyaddin, K. Y. Tan, J. P. Dehollain, R. Rahman, G. Klimeck, D. N. Jamieson, A. S. Dzurak, and A. Morello, *Phys. Rev. Lett.* **113**, 246801 (2014).
- [27] D. Becker, S. Weiss, M. Thorwart, and D. Pfannkuche, *New J. Phys.* **14**, 073049 (2012).
- [28] S. A. Gurvitz and Y. S. Prager, *Phys. Rev. B* **53**, 15932 (1996).
- [29] T. Novotný, A. Donarini, and A.-P. Jauho, *Phys. Rev. Lett.* **90**, 256801 (2003).
- [30] S. Braig and P. W. Brouwer, *Phys. Rev. B* **71**, 195324 (2005).
- [31] A. Slobodskyy, C. Gould, T. Slobodskyy, C. R. Becker, G. Schmidt, and L. W. Molenkamp, *Phys. Rev. Lett.* **90**, 246601 (2003).
- [32] C. Gould, A. Slobodskyy, D. Supp, T. Slobodskyy, P. Grabs, P. Hawrylak, F. Qu, G. Schmidt, and L. W. Molenkamp, *Phys. Rev. Lett.* **97**, 017202 (2006).
- [33] R. N. Nogueira and H. M. Petrilli, *Phys. Rev. B* **63**, 012405 (2000).
- [34] L. V. Dzemiantsova, M. Hortamani, C. Hanneken, A. Kubetzka, K. von Bergmann, and R. Wiesendanger, *Phys. Rev. B* **86**, 094427 (2012).
- [35] D. J. Griffiths, *Introduction to Electrodynamics*, 3rd ed. (Prentice Hall, Upper Saddle River, NJ, 1999).
- [36] F. Qu and P. Hawrylak, *Phys. Rev. Lett.* **95**, 217206 (2005).
- [37] J. D. Jackson, *Classical Electrodynamics*, 3rd ed. (Wiley, New York, 1999).
- [38] C. Le Gall, R. S. Kolodka, C. L. Cao, H. Boukari, H. Mariette, J. Fernández-Rossier, and L. Besombes, *Phys. Rev. B* **81**, 245315 (2010).